Calcif Tissue Int (2010) 87:144–157
DOI 10.1007/s00223-010-9368-x

LABORATORY INVESTIGATIONS

Calcium Hydroxide Promotes Cementogenesis and Induces Cementoblastic Differentiation of Mesenchymal Periodontal Ligament Cells in a CEMP1- and ERK-Dependent Manner

Francisco Wanderley Garcia Paula-Silva · Abhijit Ghosh · Higinio Arzate · Sunil Kapila · Léa Assed Bezerra da Silva · Yvonne Lorraine Kapila

Received: 23 November 2009 / Accepted: 12 April 2010 / Published online: 4 May 2010

Abstract Periodontal tissue engineering is a complex process requiring the regeneration of bone, cementum, and periodontal ligament (PDL). Since cementum regeneration is poorly understood, we used a dog model of dental pulpal necrosis and in vitro cellular wounding and mineralization assays to determine the mechanism of action of calcium hydroxide, $Ca(OH)_2$, in cementogenesis. Laser capture microdissection (LCM) followed by qRT-PCR were used to assay responses of periapical tissues to $Ca(OH)_2$ treatment. Additionally, viability, proliferation, migration, and mineralization responses of human mesenchymal PDL cells to $Ca(OH)_2$ were assayed. Finally, biochemical inhibitors and siRNA were used to investigate $Ca(OH)_2$-mediated signaling in PDL cell differentiation. In vivo, $Ca(OH)_2$-treated teeth formed a neocementum in a STRO-1- and cementum protein-1 (CEMP1)-positive cellular environment. LCM-harvested tissues adjacent to the neocementum exhibited higher mRNA levels for CEMP1, integrin-binding sialoprotein, and Runx2 than central PDL cells. In vitro, $Ca(OH)_2$ and CEMP1 promoted STRO-1-positive cell proliferation, migration, and wound closure. $Ca(OH)_2$ stimulated expression of the cementum-specific proteins CEMP1 and PTPLA/CAP in an ERK-dependent manner. Lastly, $Ca(OH)_2$ stimulated mineralization by CEMP1-positive cells. Blocking CEMP1 and ERK function abolished $Ca(OH)_2$-induced mineralization, confirming a role for CEMP1 and ERK in the process. $Ca(OH)_2$ promotes cementogenesis and recruits STRO-1-positive mesenchymal PDL cells to undergo cementoblastic differentiation and mineralization via a CEMP1- and ERK-dependent pathway.

Keywords Cementogenesis · Cementum protein-1 · STRO-1 cell-surface marker · Periodontal ligament cell · Calcium hydroxide

The authors have stated that they have no conflict of interest.

F. W. G. Paula-Silva · A. Ghosh · Y. L. Kapila (✉)
Department of Periodontics and Oral Medicine,
School of Dentistry, University of Michigan,
1011 N. University Ave., Ann Arbor, MI 48109-1078, USA
e-mail: ykapila@umich.edu

F. W. G. Paula-Silva · L. A. B. da Silva
Department of Pediatric Clinics, Preventive and Social Dentistry,
School of Dentistry of Ribeirão Preto, University of São Paulo,
Ribeirão Preto, SP, Brazil

H. Arzate
Laboratorio de Biología Periodontal y Tejidos Mineralizados,
Facultad de Odontología, Universidad Nacional Autónoma de
México, Mexico City, Mexico

S. Kapila
Department of Orthodontics and Pediatric Dentistry,
University of Michigan School of Dentistry,
Ann Arbor, MI, USA

The periodontium, defined as tissues that support and house the dentition, is comprised of root cementum, periodontal ligament (PDL), and alveolar bone [1]. Specialized cells that produce cementum and bone are thought to originate in the PDL tissue under steady-state renewal [2]. The undifferentiated mesenchymal progenitor cells within the PDL tissue capable of differentiation toward an osteoblastic or cementoblastic phenotype exhibit the mesenchymal cell-surface markers STRO-1, CD-146, and/or CD-44 [3–10]. STRO-1-positive cells are present in the mouse dental follicle and are involved in the formation of the periodontium [11, 12].

Apical periodontitis leads to the destruction of periodontal tissues. This involves the detachment of PDL fibers, concomitant with resorption of bone and cementum, and ultimately resulting in early tooth loss [13]. Using regenerative therapeutic approaches, these tissues can be restored by stimulation of PDL mesenchymal progenitor cell differentiation toward a cementoblastic or osteoblastic phenotype. Although osteoblastic differentiation has been extensively investigated, the mechanisms involved in cementoblastic differentiation remain poorly understood [2, 14, 15].

A difficulty in studying cementoblastic differentiation arises in part from the inability to identify fully differentiated cementoblasts because most molecules expressed by cementoblasts are pleiotropic and few cementum-specific markers have been described [14–18]. Cementum protein 1 (CEMP1; GenBank NM_001048212, gene ID 752014) and protein tyrosine phosphatase-like, member A/cementum attachment protein (PTPLA/CAP) are molecules expressed in PDL cells and at high levels in cementoblast-like cells and, therefore, can be considered potential local regulators of cementum metabolism and key markers of the cementoblast phenotype [11, 18–20].

Calcium hydroxide, $Ca(OH)_2$, has been widely used in dentistry to stimulate mineralization. The effects of $Ca(OH)_2$ on mineralization have been attributed to its dissociation into hydroxyl and calcium ions. Hydroxyl ions are involved in the maintenance of an alkaline environment, and calcium ions have a direct effect on extracellular matrix mineralization [21]. Furthermore, intracellular increases in calcium levels activate the calcium/calmodulin pathway, which regulates osteoblast differentiation via phosphorylation of extracellular signal-regulated kinases (ERK-1/ERK-2) and c-fos expression [22, 23]. However, a direct effect of increased extracellular calcium levels on cementoblastic differentiation has not been demonstrated. Since previous studies have demonstrated that $Ca(OH)_2$ treatment induces the deposition of a cementum-like tissue by PDL cells [24, 25], the purpose of this investigation was to evaluate the effects of increasing extracellular calcium levels on cementoblastic differentiation and cementogenesis. More specifically, we first examined cementum neogenesis in an in vivo dog model of cementogenesis and used this information to dissect the cellular and intracellular events that contribute to cementoblast differentiation, wound healing, and mineralization.

Materials and Methods

Animal Model of Pulpal Necrosis and Treatment

Animal procedures conformed to protocols reviewed and approved by the Animal Care Committee of the University of São Paulo (2007.1.191.53.0). The third and fourth mandibular premolars of six mongrel dogs (12 months of age, weighing 10–15 kg) were utilized for $Ca(OH)_2$ treatment. The animals were anesthetized intravenously with sodium thiopental (30 mg/kg body weight, Thionembutal; Abbott Laboratories, São Paulo, Brazil), and root canal access was created on the tooth surface with spherical burs. After pulp removal, the apical cementum layer was perforated, thus creating standardized apical openings as previously described [26]. The root canals were left exposed to the oral cavity for 7 days to allow microbial contamination, and then access openings were sealed with zinc oxide-eugenol cement (Dentsply Indústria e Comércio, Rio de Janeiro, Brazil). After 45 days, the development of apical periodontitis was radiographically confirmed. Root canals were instrumented to K-file #60, and a $Ca(OH)_2$ paste was used as root canal dressing (Calen; SS White Artigos Dentários, Rio de Janeiro, Brazil). A sterile cotton pellet was placed in the pulp chamber, and the access cavity was filled with zinc oxide-eugenol cement. Fifteen days later, the intracanal dressing was removed, and root canal filling was performed with gutta-percha cones and AH Plus root canal sealer (Dentsply De Trey, Konstanz, Germany).

One-hundred and eighty days after treatment, animals were killed by anesthetic overdose and blocks containing mandibular jaw bones and teeth were removed. Tissues were formalin-fixed and demineralized in 20% ethylene diamine tetraacetic acid (Sigma, St. Louis, MO). Paraffin-embedded blocks were serially sectioned, and 5-μm-thick longitudinal sections were obtained and stained with hematoxylin and eosin for histological, laser capture microdissection (LCM), or immunofluorescence analysis.

LCM and RNA Extraction

Cells from the cementoblast layer, osteoblast layer, central PDL, and newly deposited mineralized areas were isolated using LCM (Leica AS/LMD®; Leica Microsystems, Wetzlar, Germany). We harvested 9×10^3 cells per sample ($n = 5$) from teeth treated with $Ca(OH)_2$ or healthy teeth (controls). RNA was extracted from these cells using the RNeasy Micro kit (RNeasy® Micro; Qiagen, Chatsworth, CA), and RNA integrity was analyzed using a capillary electrophoresis system (Agilent 2100 BioAnalyzer; Agilent Technologies, Santa Clara, CA). In vitro transcription for total RNA amplification was performed using the TrueLabeling-PicoAMP™ kit (SABiosciences, Frederick, MD).

Quantitative Reverse Transcriptase-Polymerase Chain Reaction

Complementary DNA (cDNA) was synthesized from 1 μg of total RNA using random primers (High Quality cDNA

Reverse Transcriptase Kits; Applied Biosystems, Foster City, CA). Aliquots of 5 µl of total cDNA were amplified by quantitative reverse transcriptase-polymerase chain reaction (qRT-PCR) using the primers for CEMP1, Runt-related transcription factor 2 (Runx2), integrin-binding sialoprotein (IBSP), and bone gamma-carboxyglutamate (gla) protein (BGLAP). GAPDH was used as an internal control. Runx2, IBSP, and BGLAP primers and probes which recognize dog sequences were obtained commercially and are proprietary; thus, sequences are not available (TaqMan® Gene Expression Assay, Applied Biosystems). The CEMP1 primer sequence used was 5′-CAG GAT CCA CAT CCG TC-3′ (forward) and 5′-CTG AAC AGC TTC GAG GC-3′ (reverse). This primer recognizes the human CEMP1 sequence; the dog sequence for CEMP1 is unknown. For TaqMan® primers, amplification was done under the following conditions: denaturation at 95°C for 10 min, followed by 40 cycles of 95°C for 15 s and 60°C for 1 min. For the CEMP1 primer, amplification was done using Sybr Green (Applied Biosystems) after denaturation, followed by 40 cycles of 95°C for 15 s, 55°C for 20 s, and 72°C for 50 s. Data were analyzed using ABI Prism 7500 SDS 1.2 software (Applied Biosystems). Relative quantification was performed using the ΔΔCt method.

Cell Culture

Teeth extracted for orthodontic reasons were obtained from three healthy patients from the Department of Oral and Maxillofacial Surgery, Dental School, University of Michigan, under IRB approval. PDL cells were isolated and cultured in α-MEM as previously described [27, 28] and used from the third through fifth passages. All experiments were performed on a minimum of three independent cell isolates, and assays were performed in triplicate.

Pharmacological Treatment

PDL cells were plated at 1×10^5 cells/well in 60-mm dishes and treated with $Ca(OH)_2$ (calcium hydroxide puriss. p.a., Sigma) dissolved in either serum-free medium for short-term experiments (6–48 h) or medium supplemented with 1% FBS for long-term experiments (>72 h). For inhibitor experiments, cells were pretreated with ERK inhibitor (FR180204; EMD Chemicals, San Diego, CA), p38 inhibitor (SB203580, EMD Chemicals), and c-Jun N-terminal kinase inhibitor (SP600125, EMD Chemicals) dissolved in dimethyl sulfoxide (DMSO) or calcium channel blocker (methoxyverapamil hydrochloride, EMD Chemicals) dissolved in distilled deionized water for 1 h. Solvent controls were also examined. Then, medium was replaced with serum-free medium containing the inhibitor plus $Ca(OH)_2$.

RNA Interference

For transfection experiments, 20 or 60 pmol of ERK-1 and ERK-2 siRNA (Santa Cruz Biotechnology, Santa Cruz, CA) were used in 2×10^5 cells/well. Controls included nontargeting siRNA and no siRNA. After 36 h of transfection, cells were stimulated with $Ca(OH)_2$ as described above.

Cytotoxicity and Cell Proliferation Assays

We plated 5×10^3 cells/well in a 96-well plate, preincubated for 12 h in serum-free medium, then treated with different concentrations of $Ca(OH)_2$ for 24 h. A water-soluble tetrazolium salt, 10 µl (Dojindo, Gaithersburg, MD), was added to each well and incubated at 37°C for 3 h in the dark. After incubation, absorbance was measured at 450 nm, using a spectrophotometer, and the relative cytotoxicity was calculated. For cell proliferation assays, cell numbers were calculated against a standard curve generated from a known number of viable cells.

Wound Healing Assay

PDL cells were plated at 1×10^5 cells/well in a 96-well plate and allowed to spread and attach overnight [29]. Then, a single standardized scratch or wound was made in the center of the cell layer, and cells were treated with recombinant human CEMP1 (15 µg/ml) [18], $Ca(OH)_2$ (10 mM), a combination of both, or serum-free medium alone. Sterile-filtered CEMP1 antibody or calcium channel blocker was used to test specificity of the response. Photographs were taken immediately after wounding and 6, 12, or 18 h after treatment. The areas between the cell layer borders were measured, and percentages of wound closure were calculated.

Chemotaxis Cell Migration Assays

Chemotaxis cell migration assays were performed in transwell chambers using a fluorometric migration assay (Innocyte™ Cell Migration Assay; Calbiochem, San Diego, CA). Briefly, the lower chamber of a 96 well-plate was loaded with the chemoattractants—CEMP1, 15 µg/ml; $Ca(OH)_2$, 10 mM; a combination of both; or 10% FBS—or serum-free control medium. We resuspended 1×10^5 cells/well in serum-free medium or in serum-free medium plus calcium channel blocker (20 µM) or a CEMP1 antibody (10 µg/ml) and deposited them in the upper compartment. Plates were incubated at 37°C for 18 h. Cells that migrated to the bottom of the chamber were detached and a calcein-AM fluorescent dye was used to quantify the cells that migrated through the pores.

Immunofluorescence Staining of Cells

For immunofluorescence analysis, cells were fixed onto slides in cold methanol for 5 min, then allowed to air dry at room temperature. Slides were washed in PBS, and nonspecific binding sites were blocked with 5% bovine serum albumin (BSA, Sigma) for 30 min. Sections were then incubated with the primary antibodies for CEMP1 (polyclonal rabbit anti-CEMP1, 1:300) or STRO-1 (1:10, monoclonal mouse anti-STRO-1; R&D Systems, Minneapolis, MN) for 1 h. Then, sections were incubated with secondary antibody (1:100; goat anti-rabbit IgG Texas red–conjugated or rabbit anti-mouse IgM FITC-conjugated) for 1 h in the dark. Nuclei were counterstained by incubating slides with 4′,6-diamidino-2-phenylindole stain (DAPI, 0.5 μg/ml; Invitrogen, Carlsbad, CA) for 1 min. Slides were mounted in ProLong Gold Antifade (Molecular Probes, Eugene, OR). Rabbit IgG and mouse IgM were used as negative controls. Cells were photographed using a fluorescence microscope equipped with a digital camera. Optical densitometric analysis of intracellular protein labeling ($n = 30$/group) was performed using Image J 1.41 software (National Institutes of Health, Bethesda, MD).

Double Immunofluorescence Staining of Tissues

Tissue sections underwent antigen retrieval by boiling the slides in 10 mM sodium citrate (pH 6.0) at 90°C for 15 min. Nonspecific binding was blocked with 2% BSA for 30 min, and double immunostaining was performed by incubating sections with primary antibodies for CEMP1 (1:300) and STRO-1 (1:10) for 1 h. Then, sections were incubated with secondary antibodies (anti-rabbit IgG and antimouse IgM, 1:100). Nuclei were counterstained by incubating slides with DAPI for 1 min. Slides were mounted in ProLong Gold Antifade. The percentage of positively stained cells was evaluated in three areas of the PDL: cementoblastic area, central PDL, and osteoblastic area.

Western Blotting

Total protein content was measured in all samples using the Bradford microassay (Bio-Rad, Hercules, CA). Samples with a total protein of 10–30 μg were electrophoretically resolved using 4–12% SDS–PAGE, then electroblotted onto polyvinylidene fluoride membranes (Millipore, Billerica, MA) using standard methods. Membranes were blocked in TBS (StartingBlock™ TBS Blocking Buffer; Pierce Biotechnology, Rockford, IL) with 5% BSA for 1 h and incubated overnight with diluted primary antibodies for IBSP (1:250, Santa Cruz Biotechnology), CEMP1 (1:500), PTPLA/CAP (1:500, Santa Cruz Biotechnology), DMP1 (1:500, Santa Cruz Biotechnology), p44/42 MAPK (ERK-1/ERK-2, 1:1,000; Cell Signaling Technology, Beverly, MA), phospho-p44/42 MAPK Thr202/Tyr204 (phospho-ERK-1/ERK-2; 1:1,000; Cell Signaling Technology), and GAPDH (1:2,000, Santa Cruz Biotechnology). Secondary antibodies were anti-mouse IgG, anti-goat IgG, or anti-rabbit IgG conjugated to horseradish peroxidase (1:2,000, Santa Cruz Biotechnology). Immunoblot bands were visualized by enhanced chemiluminescence using the West-Pico ECL detection system (Pierce Biotechnology).

Alkaline Phosphatase Activity

Cells were lysed in distilled deionized water and sonicated for 15 s, and the lysate was incubated at 37°C for 30 min with ρ-nitrophenylphosphate (ρNPP; Alkaline Phosphatase Substrate, Sigma) in an alkaline phosphatase buffer solution (1.5 mM, pH 10.3; Sigma). The reaction was stopped by adding 1 N NaOH, and absorbance was read at 405 nm. Alkaline phosphatase enzymatic activity was normalized to total protein concentration.

Mineralization Assays

Mineralized nodule formation was assessed by culturing confluent PDL cells in mineralization medium for 7, 14, 21, and 28 days with changes of medium every third day. Mineralization medium consisted of α-MEM culture medium supplemented with 10 mM β-glycerophosphate, 50 μg/ml ascorbic acid, and 1% FBS. PDL cells were treated with $Ca(OH)_2$, a sterile-filtered rabbit CEMP1 antibody, an ERK-1/ERK-2 inhibitor, or mineralizing medium alone. Mineralized monolayer cell cultures were stained for matrix mineralization as described previously [10, 30]. Briefly, cultures were fixed with 70% ethanol for 10 min and stained with 2% alizarin red solution (Sigma) for 5 min at room temperature. To quantify the degree of calcium accumulation in the mineralized extracellular matrix, alizarin red–stained cultures were incubated with 100 mM cetylpyridinium chloride (Sigma) for 1 h to release calcium-bound dye into the solution. The absorbance of the released dye was measured at 570 nm using a spectrophotometer and normalized by the total protein concentration in the culture.

For dual staining with alizarin red and immunolabeling with CEMP1, cells were fixed in 70% ethanol for 1 h at 4°C. After washing in PBS, cultures were processed for immunofluorescence labeling as previously described [31].

Statistical Analysis

Quantitative data were analyzed using one-way ANOVA followed by Tukey's test ($\alpha = 0.05$).

Results

$Ca(OH)_2$-Mediated Differentiation of PDL Cells Toward a Cementoblastic Phenotype Induces Mineralized Tissue Deposition and Expression of Mineralization-Specific mRNAs In Vivo

A cementum-like tissue deposition was observed in teeth that had undergone $Ca(OH)_2$-enhanced root canal treatment. This neo-cementoid tissue was deposited in the apical foramina in contact with the $Ca(OH)_2$ paste that had been placed inside the root canals (Fig. 1a, e). A clear line demarcating the neo-cementum deposition induced by $Ca(OH)_2$ treatment was visible (Fig. 1i). The neocementum deposited in the apical foramina following root canal treatment resembles a cellular intrinsic fiber cementum, which is characterized by the entrapment of cells in the matrix. The collagen fibers are intrinsic because they do not protrude from the cementum into the PDL space. This tissue may also be formed as a reparative tissue filling resorptive and fractures defects of the root [2]. Neo-cementum formation was not observed in teeth submitted to root canal treatment without $Ca(OH)_2$ or in teeth not submitted to root canal treatment (data not shown).

In repaired teeth, cells in close contact with the newly deposited cementoid tissue stained positively for CEMP1, a marker of cementoblastic differentiation (Fig. 1b, f, j). In healthy, untreated teeth, cells adjacent to the cementum also stained positive for CEMP1 (Fig. 1n, r). Staining intensity for CEMP1 was higher in the PDL adjacent to the cementum compared to the center of the PDL in both repaired and healthy teeth. The percentage of CEMP1 positively stained cells decreased from the cementoblastic area of the PDL to the center of the PDL, with the lowest staining present toward the osteoblastic area of the PDL (Fig. 1u–w).

Since the origin of the cells lining the newly formed tissue was not known, tissues were stained for STRO-1, a marker of mesenchymal progenitor cells [3]. In the PDL of healthy and repaired teeth a higher concentration of STRO-1-positive cells was located toward the cementum and a lower number of positive cells was present toward the alveolar bone side of the PDL (Fig. 1c, g, k, o, s). We observed that STRO-1 expression was colocalized with CEMP1 expression in several cells in healthy teeth (Fig. 1p, t). In teeth subjected to root canal therapy, a higher percentage of cells close to the newly deposited cementoid tissue were double-positive (STRO-1 and CEMP1) compared to the original cementoblast layer in healthy teeth (Fig. 1d, h, l, p, t, u). Alveolar bone and osteoblasts were largely negative (Fig. 1w). Control sections incubated with anti-rabbit IgG or anti-mouse IgM were negative (data not shown). The colocalization of CEMP1- and STRO-1-positive cells close to the newly formed mineralized tissue indicates a possible relationship between CEMP1 and STRO-1 and further supports the presence of cementoblast-like progenitor cells in this reparative area.

To confirm the presence of a mineralizing cell phenotype in the apex of repaired teeth, CEMP1, IBSP, Runx2, and BGLAP mRNA expression was evaluated in the cells of this area by LCM and qRT-PCR. Higher CEMP1 mRNA expression was observed in the cementoblastic area of the PDL and in the center of the PDL compared to the osteoblastic area of the PDL (Fig. 2a). Furthermore, in repaired teeth CEMP1 mRNA expression was significantly higher in the cementoblastic region of the PDL compared to healthy teeth. IBSP and BGLAP mRNA expression was similar in the cementoblastic and osteoblastic areas in both repaired and healthy teeth, indicating a mineralizing cell phenotype close to the newly formed mineralized tissue (Fig. 2b, c). Similarly, Runx2 transcripts were expressed in higher amounts in cells adjacent to the cementum and bone compared to cells in the center of the PDL, with cells adjacent to the cementum in repaired teeth expressing significantly more Runx2 than healthy teeth (Fig. 2d). Taken together, the higher mRNA and protein expression for mineralization-associated proteins observed in the reparative areas close to the newly formed cementoid tissue indicates a cementoblastic phenotype for cells present in repaired teeth.

CEMP1 Promotes PDL Cell Proliferation, Migration, and Mineralization

Since CEMP1 expression was colocalized with STRO-1-positive cells and higher CEMP1 expression was observed in the cementoblastic area in teeth treated with $Ca(OH)_2$, we investigated whether CEMP1 or $Ca(OH)_2$ is a chemotactic factor for STRO-1-positive cells. Relative to serum-free media alone, recombinant human CEMP1, $Ca(OH)_2$, or a combination of the two stimulated PDL cell migration and wound closure at 18 h after treatment. $Ca(OH)_2$ and CEMP1 together promoted faster cell migration at 6 and 12 h compared to treatment with $Ca(OH)_2$ alone. Blocking calcium channels or CEMP1 activity prevented cell migration, confirming the role of both in wound closure in vitro (Fig. 3a). A chemotactic cell migration assay further confirmed these results (Fig. 3b).

A higher percentage of migrating cells were STRO-1-positive under CEMP1 vs. $Ca(OH)_2$ stimulation in the wound healing assays at 18 h (Fig. 3c). The combined treatment of CEMP1 and $Ca(OH)_2$ maintained a proportion of STRO-1-positive cells within the migrating cells at levels similar to those induced by CEMP1 alone.

CEMP1 treatment stimulated higher levels of cell proliferation than the serum-free control 6–72 h after

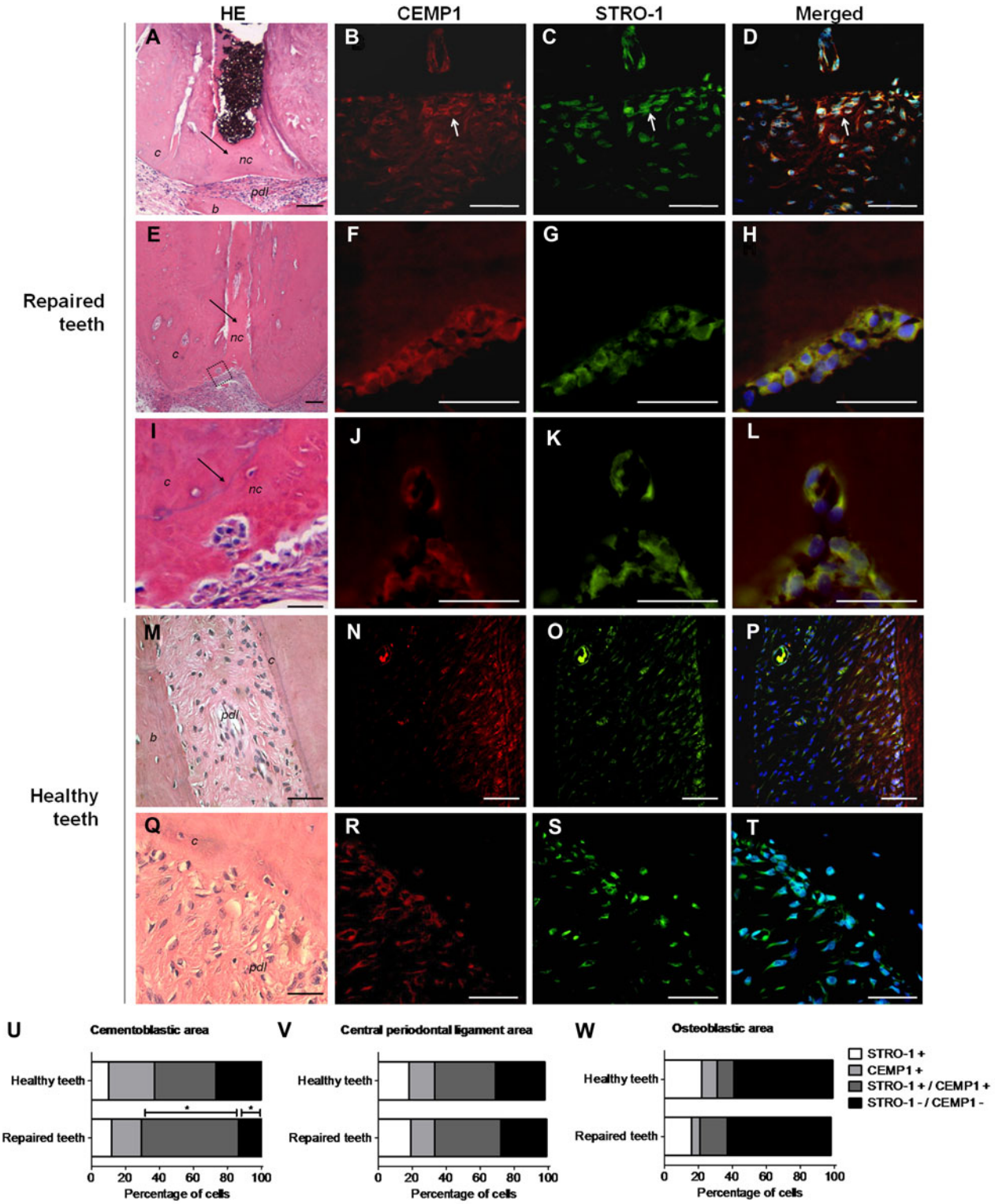

Fig. 1 Neocementum tissue (*nc*) deposited in repaired teeth (**a**, **e**, **i** *arrows*; **i** higher magnification of **e**). Cells lining the neocementum were immunopositive for CEMP1 (**b**, **f**, **j**) and STRO-1 (**c**, **g**, **k**). Cementum (*c*), periodontal ligament (*pdl*), and bone (*b*) from healthy teeth were used as controls (**m**–**t**). * $P < 0.05$ compared to healthy cementoblast, $n = 5$, bar = 50 μm. **u**–**w** Relative expression of specified markers

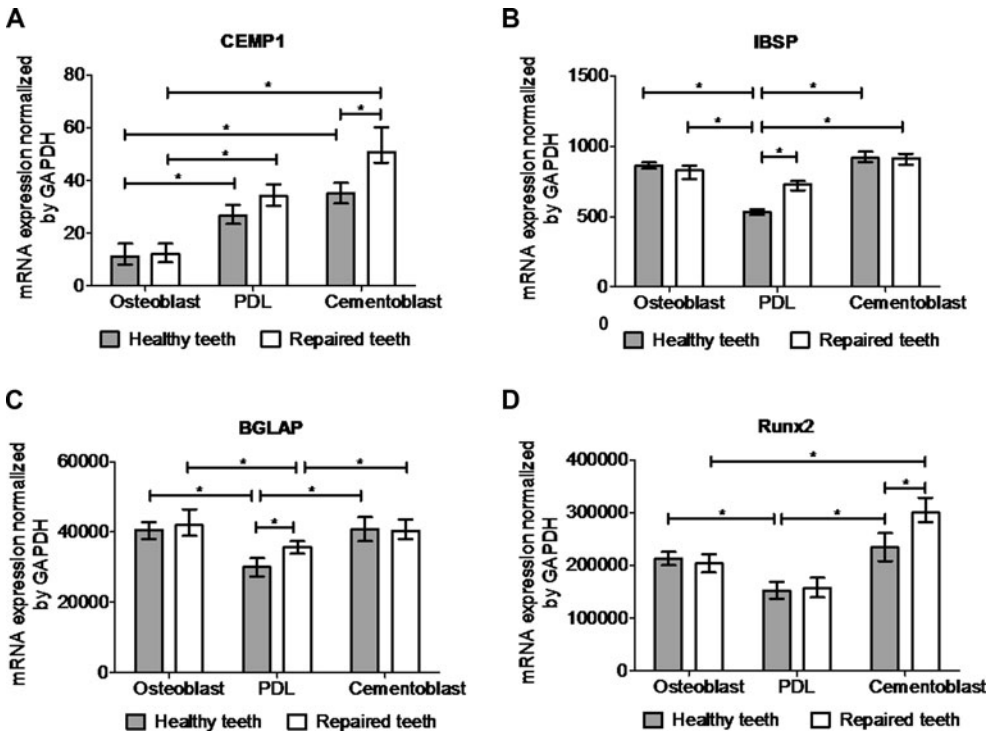

Fig. 2 Cells from the cementoblastic, central, and osteoblastic areas of the PDL were harvested by LCM; mRNA was isolated; and expression of CEMP1 (**a**), IBSP (**b**), BGLAP (**c**), and Runx2 (**d**) was determined by qRT-PCR. GAPDH was used as an internal control. * $P < 0.05$, $n = 5$

treatment. In contrast, relative to control treatment, $Ca(OH)_2$ did not affect cell proliferation up to 36 h but inhibited cell proliferation at 48–72 h of culture (Fig. 3d). CEMP1 and $Ca(OH)_2$ treatment combined stimulated cell proliferation up to 36 h; however, after that, cell proliferation was not different from the control. Together, these findings suggest different roles for CEMP1 and $Ca(OH)_2$ in the reparative phenomenon observed in vivo.

To further investigate if CEMP1 is involved in mineralization by PDL cells as it is for other cells [32, 33], we induced PDL cell mineralization using β-glycerophosphate and ascorbic acid with or without $Ca(OH)_2$ in the presence or absence of a CEMP1 function–blocking antibody. Cells in control medium retained their characteristic spindle-shaped morphology, while cells maintained in elevated levels of calcium in mineralizing medium lost their initial fibroblastic spindle-shaped morphology and exhibited shorter spindles and an oval-shaped morphology (Fig. 4a). Changes in PDL cell morphology combined with increased expression of mineralization-associated proteins have been considered indicators of osteoblastic/cementoblastic lineage differentiation [34]. Thus, the morphological changes observed in our PDL cell cultures under high calcium levels may be indicative of cementoblastic lineage differentiation.

$Ca(OH)_2$-treated cells had greater numbers of mineralized nodules compared to cells cultured in mineralization medium alone (Fig. 4b). The cells around the nodules in both conditions were CEMP1-positive; however, staining intensity was highest in $Ca(OH)_2$-treated cells (Fig. 4a, b). At a distance from the nodules, cells were CEMP1-negative under treatment with mineralization medium alone, whereas all cells were CEMP1-positive under treatment with $Ca(OH)_2$ in mineralization medium (Fig. 4b [c, f]).

The highest level of mineralization was observed when $Ca(OH)_2$ was added to the mineralization medium (Fig. 4c). However, when cells were incubated with a CEMP1 blocking antibody, less mineralization was observed under all conditions. Blocking CEMP1 activity in cells treated with $Ca(OH)_2$ diminished mineralized nodule formation. Cells incubated with regular medium did not show nodule formation, and cells incubated in mineralization medium plus rabbit IgG exhibited similar nodule formation as cells incubated with mineralization medium alone.

Increase in Extracellular Calcium Levels Upregulates Expression of Cementoblast-Related Proteins and Mineralization

To further understand the role of $Ca(OH)_2$ in PDL cell differentiation, we evaluated the ability of PDL cells to express mineralization-associated proteins upon treatment with $Ca(OH)_2$. PDL cells were treated with 1–20 mM of

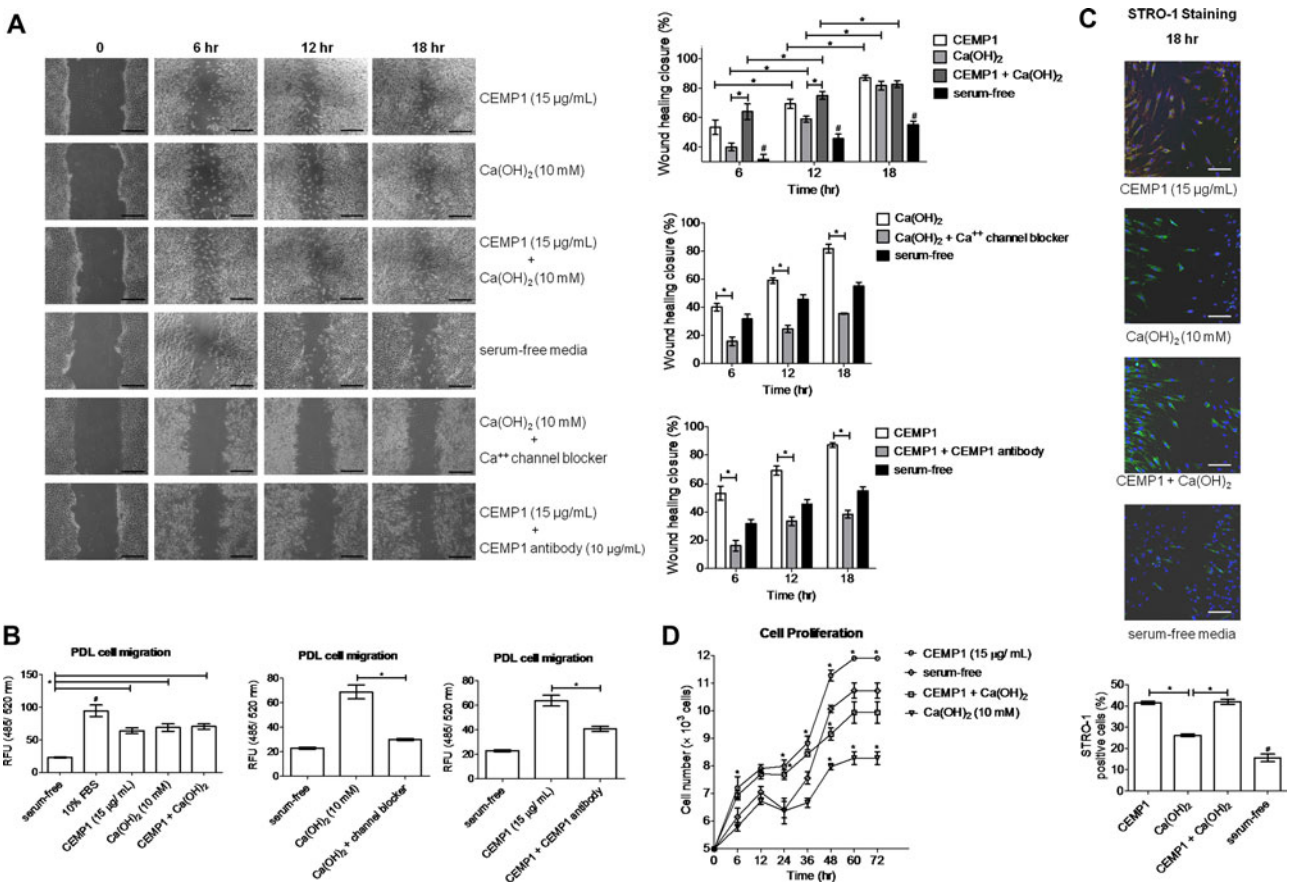

Fig. 3 **a** Wounding assay was used to evaluate cell migration. Bar = 500 µm, $n = 3$. **b** Cell migration was confirmed using a fluorescence quantitative assay, $n = 6$. **c** The percentage of STRO-1-positive cells in **a** was calculated. Bar = 50 µm, $n = 6$. **d** Cell proliferation, $n = 3$. * $P < 0.05$ compared to indicated bar, # $P < 0.05$ compared to all other treatments

$Ca(OH)_2$ diluted in regular serum-free medium for 24 h (Fig. 5a). A dose-dependent decrease in cell viability was observed with increasing concentrations of $Ca(OH)_2$. Doses lower than 15 mM permitted cell viability of 90% or greater, and therefore, subsequent experiments were performed with concentrations lower than that.

Different concentrations of $Ca(OH)_2$ stimulated varied expression of mineralization-associated proteins in PDL cells. Basal PTPLA/CAP expression was detected at 6, 12, and 24 h in PDL cells, and $Ca(OH)_2$ treatment had minimal effects on PTPLA/CAP expression in short-term cultures (Fig. 5b). However, in long-term cultures, PTPLA/CAP expression was induced by $Ca(OH)_2$ at 3, 7, and 14 days of culture; and the most robust effects were exhibited with the higher concentrations of $Ca(OH)_2$ tested (Fig. 5c).

CEMP1 expression was induced 12 h following treatment with $Ca(OH)_2$, but no expression was detected in the control. At 24 h, the induction of CEMP1 at lower doses of $Ca(OH)_2$ was comparable to basal expression levels, while 10 mM $Ca(OH)_2$ induced a slight increase in CEMP1 expression (Fig. 5b). As seen for PTPLA/CAP in long-term cultures, $Ca(OH)_2$ substantially induced CEMP1 expression in PDL cells at 3, 7, and 14 days of culture. At 14 days, CEMP1 expression was higher for $Ca(OH)_2$-treated cells compared to those in regular media, irrespective of the dose used (Fig. 5c). Similar expression profiles were noted for dentin matrix protein 1 (DMP1).

$Ca(OH)_2$ exerted little effect on basal IBSP expression at 6, 12, and 24 h of culture (Fig. 5b). At 3 and 7 days a dose-dependent increase in IBSP expression was observed in cells treated with $Ca(OH)_2$, although at 14 days no difference was observed in IBSP expression between $Ca(OH)_2$-treated cells and controls (Fig. 5c).

To further investigate the mineralizing phenotype induced by $Ca(OH)_2$, alkaline phosphatase activity was measured at 7 and 14 days (Fig. 5d). Relative to cells cultured in mineralizing medium, cells in mineralizing medium containing $Ca(OH)_2$ had higher alkaline phosphatase activity at 7 and 14 days in culture. $Ca(OH)_2$ in regular medium did not induce increases in alkaline phosphatase activity.

While cells treated with mineralization medium alone exhibited no nodule formation on days 14 and 21 of

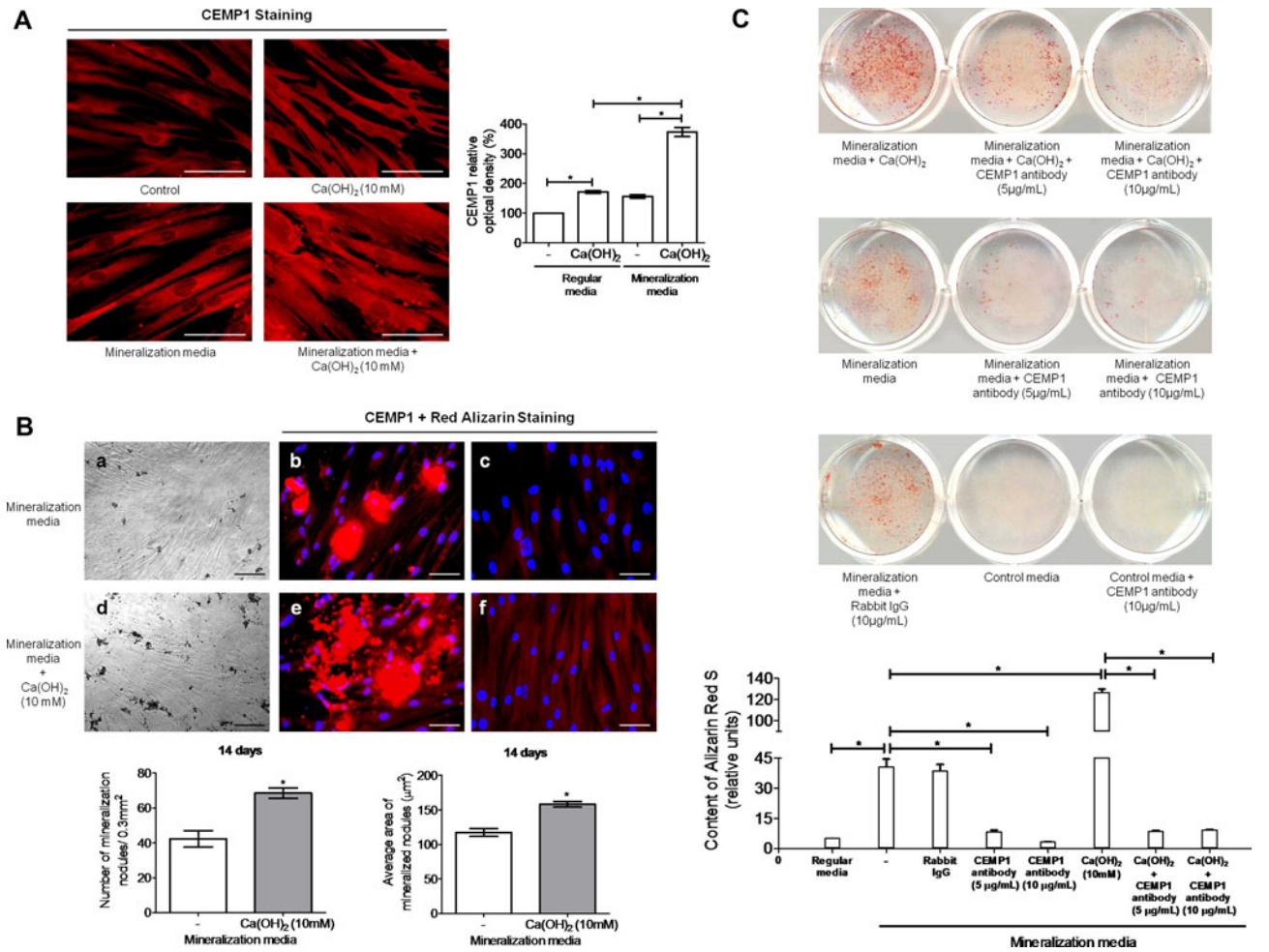

Fig. 4 **a** Intensity of CEMP1 fluorescence. Bar = 15 μm, $n = 30$. **b** Mineralized nodules (*a, d*; bar = 100 μm) were stained and pictures taken of areas adjacent to (*b, e*) and distant from (*c, f*) the nodules. Bar = 20 μm, $n = 3$. **c** Cells were cultured in medium with $Ca(OH)_2$, and CEMP1 activity was blocked using an antibody; $n = 3$, * $P < 0.05$

culture, $Ca(OH)_2$ enhanced mineralized nodule formation at these time points (Fig. 5e). On day 28, $Ca(OH)_2$ produced a dose-dependent increase in mineralized nodule formation. Therefore, $Ca(OH)_2$ stimulated the expression of mineralization-associated proteins, alkaline phosphatase activity, and mineralization to a higher level than controls not treated with $Ca(OH)_2$. These findings demonstrate the important role of $Ca(OH)_2$ in inducing cementoblastic differentiation of PDL cells.

Increased Extracellular Calcium Mediates Cementum-Specific Protein Expression Via ERK MAPK Signaling

The mechanisms involved in regulating cementum-associated proteins due to elevation of extracellular calcium have not been explored. Thus, we investigated the role of $Ca(OH)_2$ in the regulation of PTPLA/CAP and CEMP1, proteins considered to be cementoblast-specific [18, 35, 36]. In addition, since mitogen-activated protein kinases mediate cementum-related protein expression in cementoblasts [37], we inhibited the extracellular signal–regulated kinase, p38, and c-Jun N-terminal kinase pathways, using chemical inhibitors to determine if these kinases are involved in cementoblastic differentiation of PDL cells. Treatment with $Ca(OH)_2$ elevated CEMP1 and PTPLA/CAP levels, as previously demonstrated. The ERK inhibitor blocked CEMP1 and PTPLA/CAP expression, whereas p38 and JNK inhibitors did not (Fig. 6a), indicating that $Ca(OH)_2$ mediates CEMP1 and PTPLA/CAP expression via the ERK signaling pathway. To further examine the role of ERK signaling in this mechanism, time-dependent experiments were performed to assess ERK phosphorylation. $Ca(OH)_2$ treatment stimulated ERK-1 and ERK-2 phosphorylation time-dependently, with phosphorylation peaking at 30–45 min and decreasing thereafter. Longer-term evaluation confirmed the cycling pattern of ERK phosphorylation upon $Ca(OH)_2$ treatment (Fig. 6b). Total ERK levels remained unchanged.

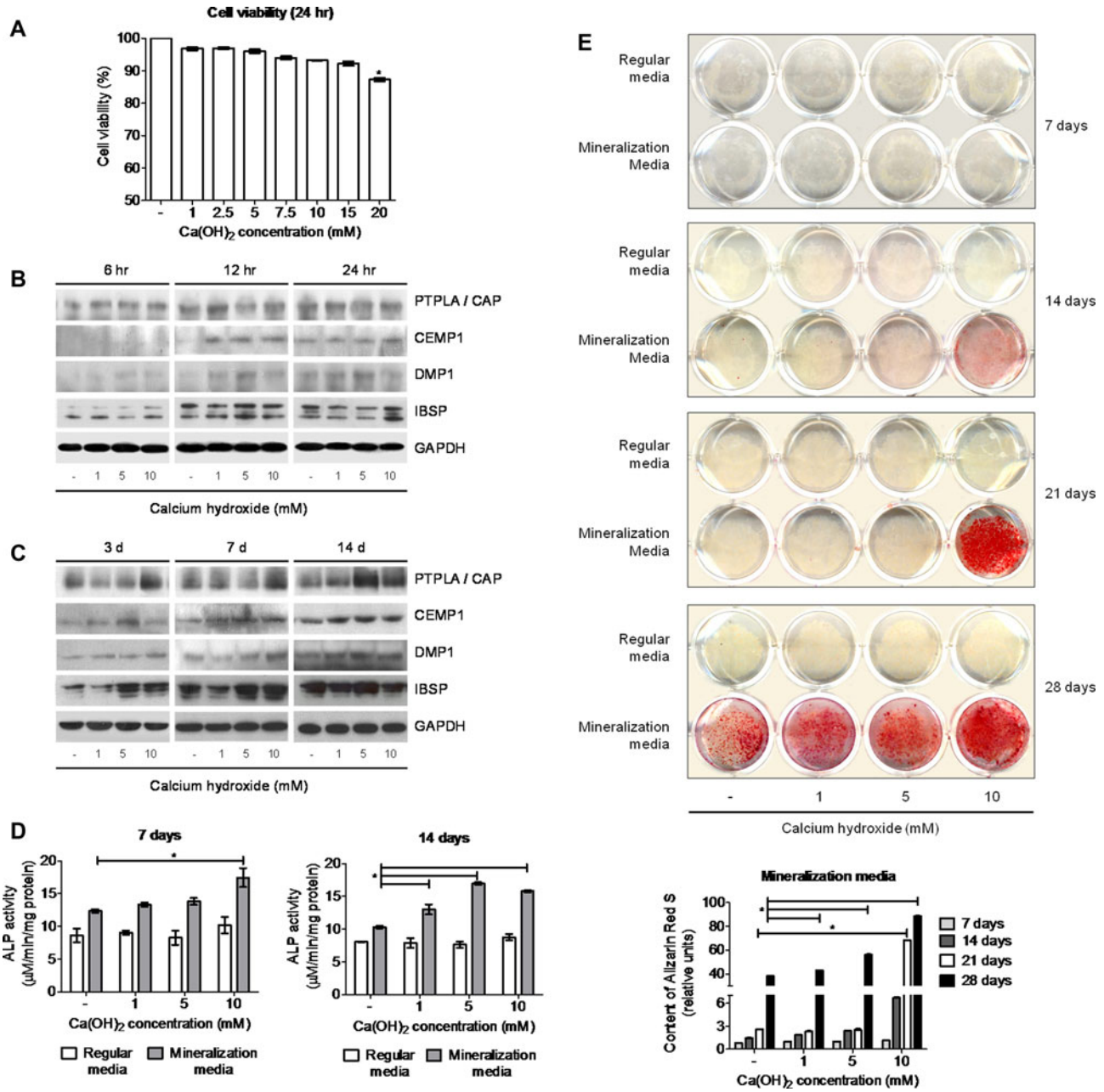

Fig. 5 **a** Cell viability after treatment with $Ca(OH)_2$, $n = 3$. Cell cultures were stimulated with $Ca(OH)_2$ for **b** short or **c** long term. Expression of CEMP1 (50 kDa), PTPLA/CAP (56 kDa), DMP1 (57 kDa), IBSP (70 kDa), and GAPDH (37 kDa) proteins was determined; $n = 3$. **d** Alkaline phosphatase activity, $n = 3$. **e** Mineralized nodule formation, $n = 3$, * $P < 0.05$

To confirm that PTPLA/CAP and CEMP1 regulation is mediated via ERK, ERK-1 and ERK-2 expression was inhibited using siRNA (Fig. 6c). Treatment with ERK-1 and ERK-2 siRNA downregulated PTPLA/CAP and CEMP1 expression. Furthermore, simultaneous suppression of ERK-1/ERK-2 and stimulation with $Ca(OH)_2$ resulted in diminished levels of PTPLA/CAP and CEMP1 expression compared to $Ca(OH)_2$ stimulation alone. Inhibition of ERK-1/ERK-2 using a biochemical inhibitor also blocked the increased mineralization induced by $Ca(OH)_2$ (Fig. 6d).

Since ERK is phosphorylated in response to ionomycin-induced intracellular calcium increases [38], we examined whether ERK phosphorylation in PDL cells is mediated directly by entrance of calcium into the cells. To this end, we used a general calcium channel blocker and treated the cells with $Ca(OH)_2$. Blocking calcium channels in the presence of $Ca(OH)_2$ diminished the levels of ERK

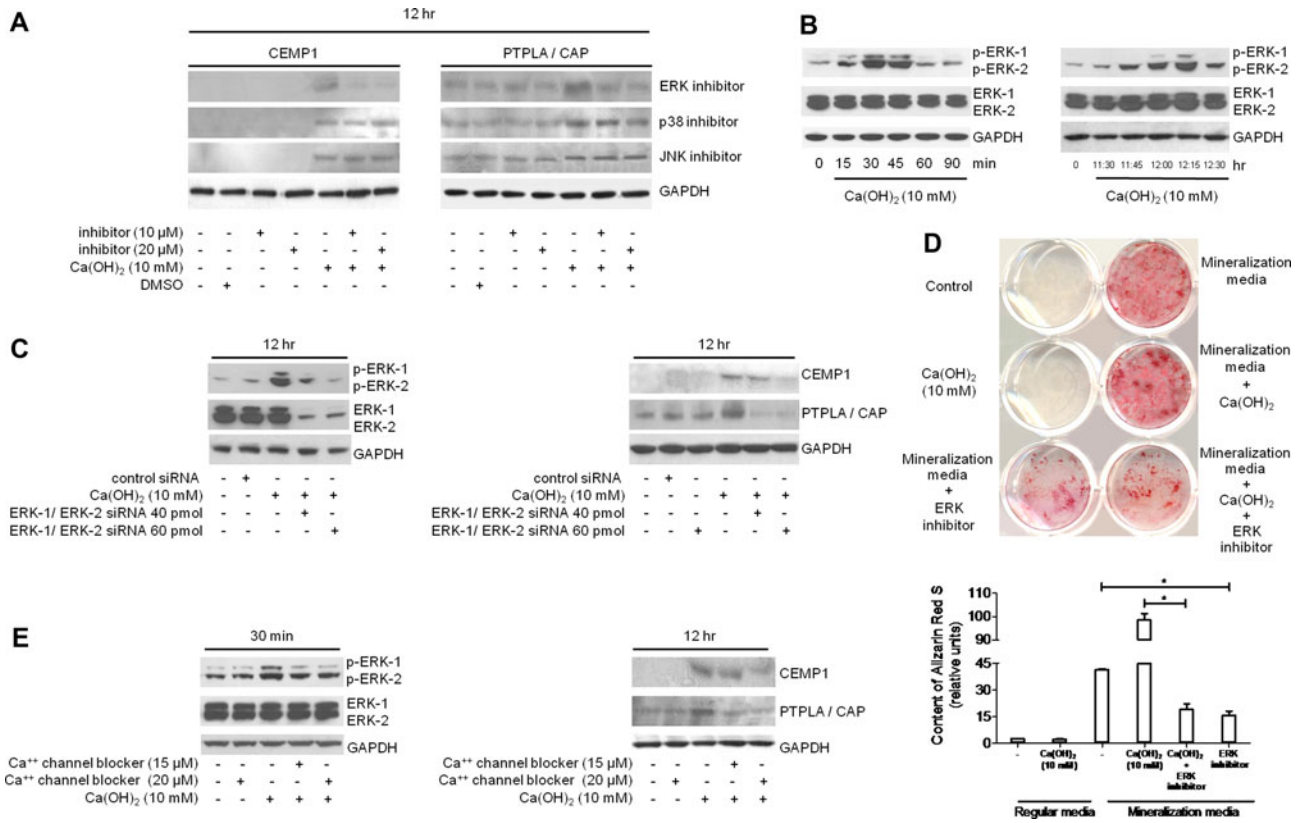

Fig. 6 **a** Cells were treated with MAPK inhibitors, and protein expression was examined. **b** Effects of $Ca(OH)_2$ on ERK-1/ERK-2 (44 and 42 kDa) phosphorylation. **c** ERK-1/ERK-2 siRNA effects on $Ca(OH)_2$-mediated PTPLA/CAP and CEMP1 expression. **d** Effects of ERK inhibition on mineralization. $n = 3$, * $P < 0.05$. **e** Effects of a calcium channel blocker on ERK-1/ERK-2 phosphorylation and protein expression

phosphorylation compared to cells treated with $Ca(OH)_2$ alone. Treatment with a calcium channel blocker for 12 h led to a dose-dependent decrease in CEMP1 expression and lower PTPLA/CAP expression (Fig. 6e).

Discussion

Achieving complete periodontal regeneration is challenging because several tissues require regeneration. One of those complex tissues is cementum, a tissue important for anchoring PDL fibers. PDL cells can form mineralized nodules in vitro and express mineralization-associated proteins [10, 39, 40]. Thus, the PDL is thought to contain cells that are at different stages of differentiation and lineage commitment and that could potentially contribute to cementogenesis. We demonstrate for the first time that increasing extracellular calcium levels leads specifically to cementoblastic differentiation of PDL cells and mineralization in vitro and in vivo. Additionally, our findings provide new information on the role of CEMP1 in PDL mesenchymal cell recruitment, proliferation, and mineralization (Fig. 7).

In vivo, CEMP1- and STRO-1-positive cells were colocalized adjacent to the root surface in areas where neo-cementum was deposited, suggesting that the cells that deposited the reparative cementum were of mesenchymal origin. In vitro, treatment of PDL cells with CEMP1 protein stimulated the proliferation and migration of PDL cells, with the migration front comprised of STRO-1-positive cells. Our findings are consistent with other reports showing that STRO-1-positive cells are located next to the cementum [4], although an overlap between CEMP1- and STRO-1-expressing cells has not been previously described.

CEMP1 is a likely mediator in wound healing and periodontal regeneration since it stimulates PDL cell proliferation and migration. CEMP1 leads to migration of STRO-1-positive cells, suggesting a possible mechanism for the recruitment of mesenchymal cells toward a CEMP1 signal. The role of CEMP1 as a chemoattractant and as a promoter of mineralization is further supported by the findings that mineralization is reduced upon blocking CEMP1 function in vitro, and cells in direct contact with neo-cementum induced by $Ca(OH)_2$ are CEMP1-positive in vivo. In cementoblastoma cells, blocking CEMP1

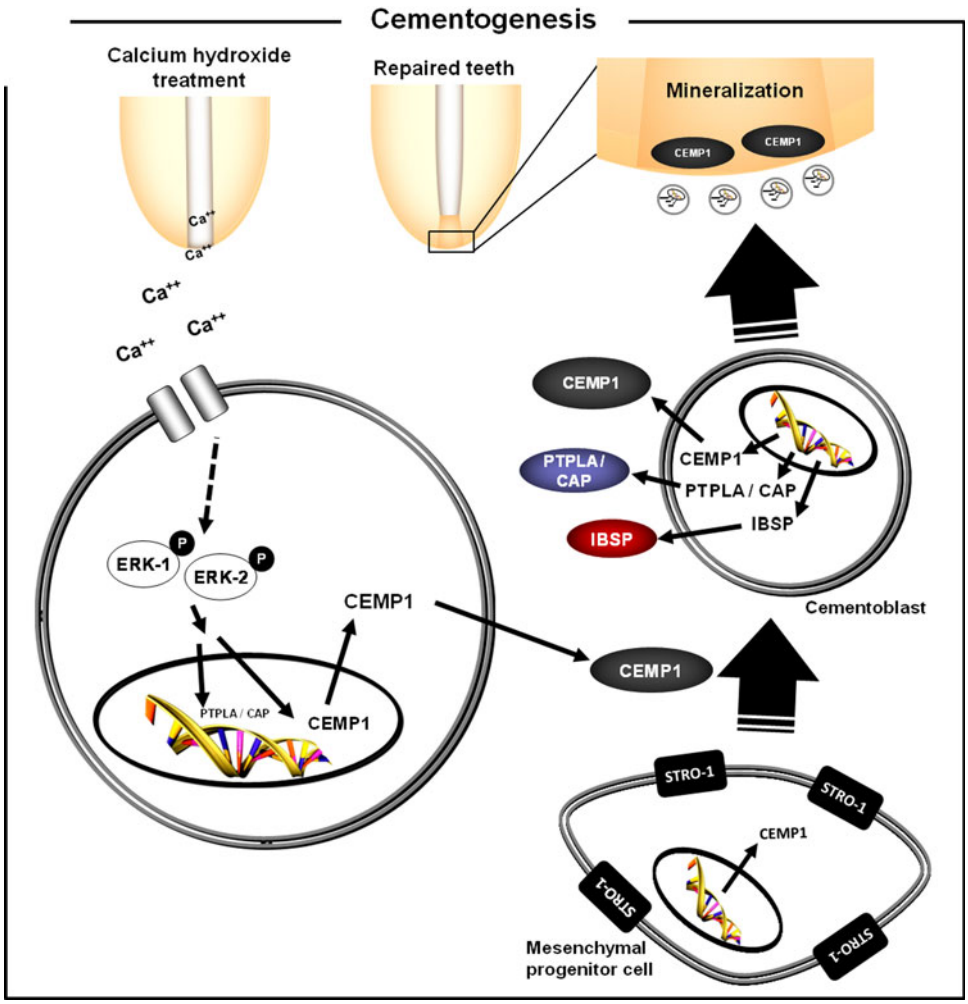

Fig. 7 Proposed model of CEMP1-ERK-mediated cementogenesis in response to $Ca(OH)_2$. $Ca(OH)_2$ induces increased extracellular calcium levels and expression of PTPLA/CAP and CEMP1 via ERK MAPK signaling. CEMP1 recruits STRO-1-positive progenitor mesenchymal cells and together with calcium hydroxide mediates migration, proliferation, and differentiation of PDL cells toward a cementoblastic phenotype

activity decreases alkaline phosphatase activity, IBSP, and osteopontin expression without altering cell proliferation and viability [32]. Transfection of CEMP1 into human gingival fibroblasts, cells that normally do not express CEMP1, led to the development of a cementoblastic phenotype in these cells. Specifically, these cells expressed alkaline phosphatase, IBSP, PTPLA/CAP, BGLAP, osteopontin, and Runx2 and underwent mineralization [33, 41]. Recombinant human CEMP-1 strongly cross-reacts with antibodies against collagen type X but not with antibodies against type I. Furthermore, amino acids 30–110 in the CEMP1 sequence show 40% similarity with type X human collagen. Nevertheless, CEMP1 does not have the characteristic collagen-like gly-x–y repeats, which suggests that CEMP1 is not a true collagen [18]. Although PTPLA/CAP has been used as a marker of cementoblastic differentiation, the sequence AY455942 deposited in public databanks for human PTPLA may not represent CAP detected in teeth [42]. In our studies we used a commercially available mouse monoclonal antibody raised against cementum attachment protein of cow origin.

Calcium is a well-known regulator of transcriptional gene expression in osteoblasts, and many cellular responses to calcium signals are modulated by calcium/calmodulin-dependent enzymes [23], although the role of calcium in cementoblastic differentiation is not known. In osteoblasts, intracellular increases in calcium levels activate calmodulin, which binds to and activates calcium/calmodulin-dependent protein kinase II and downstream phosphorylates ERK-1/ERK-2. ERK-1/ERK-2 are important intermediary signaling molecules for osteoblastic gene expression via regulation of c-*fos* [22]. Here, we demonstrated that blocking calcium channels in the presence of increased extracellular calcium levels prevents ERK-1/ERK-2 phosphorylation and PTPLA/CAP and CEMP1 expression. Silencing ERK-1/ERK-2 gene expression confirmed the role of this intermediate pathway in cementoblastic differentiation under $Ca(OH)_2$ treatment. Although calcium ion-mediated increases in pH could have potentially influenced cell differentiation, the buffering capacity of the medium following incubation in a 5% CO_2 atmosphere reduced this effect. The pH of the medium was consistently maintained

at 7.4 following CO_2 incubation. A pH of 7.4 was the regular α-MEM pH value used in our studies. Therefore, our results can be attributed to raising local calcium concentrations rather than increasing pH levels. Furthermore, the use of a calcium channel blocker prevented CEMP1 and PTPLA/CAP expression, demonstrating the role of calcium ions in this process.

Molecules responsible for recruiting mesenchymal cells and inducing their differentiation into cementoblasts have not been identified. Our results provide evidence that CEMP1 could be one of the molecules that performs these functions. STRO-1-positive PDL cells transplanted into artificially created PDL defects in immunocompromised rats induced the deposition of a layer of cementum tissue [3]. Also, human PDL cells transplanted with a β-tricalcium phosphate scaffold into the subcutaneous dorsal surface of mice induced a mineralized tissue deposition on the surface of the scaffold, and these tissues exhibited upregulated gene expression for BGLAP, IBSP, CEMP1, and periostin, unlike controls [8]. Our findings are in agreement with these previous publications since we demonstrate that a cementum-like tissue was induced in the dental root apex of repaired teeth and that cells lining this tissue were double-stained for STRO-1 and CEMP1. These data further suggest that clinical treatment with $Ca(OH)_2$ recruits mesenchymal, STRO-1-positive PDL cells via a CEMP1 gradient that promotes mesenchymal cell differentiation toward cementogenesis in an ERK-dependent manner.

Conclusions

$Ca(OH)_2$-mediated increases in extracellular calcium levels induced cementoblastic differentiation of PDL cells by an ERK-dependent mechanism. Blocking calcium channels inhibited ERK phosphorylation and thereby prevented cementoblast-specific protein expression (PTPLA/CAP and CEMP1). Ultimately, CEMP1 and ERK upregulation was central to cementogenesis since blocking their functions abolished mineralization.

Acknowledgements This study was supported by NIH-RO1-DE13725 (to Y. L. K.) and NIH-RO1-DE16671 (to S. K.). F. W. G. P.-S. received fellowships from the PTPLA/CAPES Foundation (0668/07-9) and the State of São Paulo Research Foundation (FAPESP 06/51161-0).

References

1. Nanci A, Bosshardt DD (2006) Structure of periodontal tissues in health and disease. Periodontol 2000 40:11–28
2. Bosshardt DD (2005) Are cementoblasts a subpopulation of osteoblasts or a unique phenotype? J Dent Res 84:390–406
3. Seo B-M, Miura M, Gronthos S, Bartold PM, Batouli S, Brahim J, Young M, Robey PG, Wang C-Y (2004) Investigation of multipotent postnatal stem cells from human periodontal ligament. Lancet 364:149–155
4. Chen SC, Marino V, Gronthos S, Bartold PM (2006) Location of putative stem cells in human periodontal ligament. J Periodont Res 41:547–553
5. Nagatomo K, Komaki M, Sekiya I, Sakaguchi Y, Oda S, Muneta T, Ishikawa I (2006) Stem cell properties of human periodontal ligament cells. J Periodont Res 41:303–310
6. Gay IC, Chen S, MacDougall M (2007) Isolation and characterization of multipotent human periodontal ligament stem cells. Orthod Craniofacial Res 10:149–160
7. Jo Y-Y, Lee H-J, Kook S-Y, Choung H-W, Park J-Y, Chung J-H, Choung Y-H, Kim E-S, Yang H-C, Choung P-H (2007) Isolation and characterization of postnatal stem cells from human dental tissues. Tissue Eng 13:767–773
8. Fujii S, Maeda H, Wada N, Tomokiyo A, Saito M, Akamine A (2008) Investigating a clonal human periodontal ligament progenitor/stem cell line in vitro and in vivo. J Cell Physiol 215:743–749
9. Lin N-H, Menicanin D, Mrozik K, Gronthos S, Bartold PM (2008) Putative stem cells in regenerating human periodontium. J Periodontol Res 43:514–523
10. Xu J, Wang W, Kapila Y, Lotz J, Kapila S (2009) Multiple differentiation PTPLA/CAPacity of STRO-1^+/$CD146^+$ PDL mesenchymal progenitor cells. Stem Cells Dev 18:487–496
11. Kémoun P, Laurencin-Dalicieux S, Rue J, Vaysse F, Roméas A, Arzate H, Conte-Auriol F, Farges JC, Salles JP, Brunel G (2007) Localization of STRO-1, BMP-2/-3/-7, BMP receptors and phosphorylated Smad-1 during the formation of mouse periodontium. Tissue Cell 39:257–266
12. Kémoun P, Laurencin-Dalicieux S, Rue J, Farges J-C, Gennero I, Conte-Auriol F, Briand-Mesange F, Gadelorge M, Arzate H, Narayanan S, Brunel G, Salles J-P (2007) Human dental follicle cells acquire cementoblast features under stimulation by BMP-2/-7 and enamel matrix derivatives (EMD) in vitro. Cell Tissue Res 329:283–294
13. Márton IJ, Kiss C (2000) Protective and destructive immune reactions in apical periodontitis. Oral Microbiol Immunol 15:139–150
14. Saygin NE, Giannobile WV, Sommerman MJ (2000) Molecular and cell biology of cementum. Periodontol 2000 24:73–98
15. Grzesik WJ, Narayanan AS (2002) Cementum and periodontal wound healing and regeneration. Crit Rev Oral Biol Med 13:474–484
16. Foster BL, Sommerman MJ (2005) Regenerating the periodontium: is there a magic formula? Orthod Craniofacial Res 8:285–291
17. Gonçalves PF, Sallum EA, Casati MZ, Toledo S, Nociti FH Jr (2005) Dental cementum reviewed: development, structure, composition, regeneration and potential functions. Braz J Oral Sci 4:651–658
18. Álvarez-Pérez MA, Narayanan S, Zeichner-David M, Rodríguez-Carmona B, Arzate H (2006) Molecular cloning, expression and immunolocalization of a novel human cementum-derived protein (CP-23). Bone 38:409–419
19. Arzate H, Jiménez-García LF, Álvarez-Perez MA, Landa A, Bar-Kana I, Pitaru S (2002) Immunolocalization of a human cementoblastoma-conditioned medium-derived protein. J Dent Res 81:541–546
20. Kitagawa M, Tahara H, Kitagawa S, Oka H, Kudo Y, Sato S, Ogawa I, Miyaichi M, Takata T (2006) Characterization of established cementoblast-like cell lines from human cementum-lining cells in vitro and in vivo. Bone 39:1035–1042
21. Fava LR, Saunders WP (1999) Calcium hydroxide pastes: classification and clinical indications. Int Endod J 32:257–282

22. Zayzafoon M, Fulzele K, McDonald JM (2005) Calmodulin and calmodulin-dependent kinase IIα regulate osteoblast differentiation by controlling *c-fos* expression. J Biol Chem 280:7049–7059
23. Zayzafoon M (2006) Calcium/calmodulin signaling controls osteoblast growth and differentiation. J Cell Biochem 97:56–70
24. Leonardo MR, Silva LA, Leonardo RT, Utrilla LS, Assed S (1993) Histological evaluation of therapy using a calcium hydroxide dressing for teeth with incompletely formed apices and periapical lesions. J Endod 19:348–352
25. Leonardo MR, Hernandez ME, Silva LA, Tanomaru-Filho M (2006) Effect of a calcium hydroxide-based root canal dressing on periapical repair in dogs: a histological study. Oral Surg Oral Med Oral Pathol Oral Radiol Endod 102:680–685
26. Paula-Silva FWG, Hassan B, Silva LAB, Leonardo MR, Wu M-K (2009) Outcome of root canal treatment in dogs determined by periapical radiography and cone-beam computed tomography scans. J Endod 35:723–726
27. Kapila YL, Kapila S, Johnson PW (1996) Fibronectin and fibronectin fragments modulate the expression of proteinases and proteinase inhibitors in human periodontal ligament cells. Matrix Biol 15:251–261
28. Paula-Silva FWG, Ghosh A, Silva LAB, Kapila YL (2009) TNF-α induces an odontoblastic phenotype in dental pulp cells. J Dent Research 88:339–344
29. Kapila YL, Niu J, Johnson PW (1997) The high affinity heparin-binding domain and the V region of fibronectin mediate invasion of human oral squamous cell carcinoma cells in vitro. J Biol Chem 272:18932–18938
30. Wang W, Xu J, Kirsch T (2003) Annexin-mediated Ca^{2+} influx regulates growth plate chondrocyte maturation and apoptosis. J Biol Chem 278:3762–3769
31. Oliveira PT, Zalzal SF, Beloti MM, Rosa AL, Nanci A (2007) Enhancement of in vitro osteogenesis on titanium by chemically produced nanotopography. J Biomed Mater Res A 80:554–564
32. Álvarez-Pérez MA, Pitaru S, Álvarez-Fregoso O, Reyes-Gasga J, Arzate H (2003) Anti-cementoblastoma-derived protein antibody partially inhibits mineralization on a cementoblastic cell line. J Struct Biol 143:1–13
33. Carmona-Rodríguez B, Álvarez-Pérez MA, Narayanan S, Zeichner-David M, Reyes-Gasga J, Molina-Guarneros J, García-Hernández AL, Suárez-Franco JL, Chavarría IG, Villareal-Ramírez E, Arzate H (2007) Human cementum protein 1 induces expression of bone and cementum proteins by human gingival fibroblasts. Biochem Biophys Res Commun 358:763–769
34. Yang ZH, Zhang XJ, Dang NN, Ma ZF, Xu L, Wu JJ, Sun Y-J, Duan Y-Z, Lin Z, Jin Y (2009) Apical tooth germ cell-conditioned medium enhances the differentiation of periodontal ligament stem cells into cementum/periodontal ligament-like tissues. J Periodontal Res 44:199–210
35. Arzate H, Olson SW, Page RC, Gown AM, Narayanan AS (1992) Production of a monoclonal antibody to an attachment protein derived from human cementum. FASEB J 11:2990–2995
36. BarKana I, Narayanan AS, Grosskop A, Savion N, Pitaru S (2000) Cementum attachment protein enriches putative cementoblastic populations on root surfaces in vitro. J Dent Res 79: 1482–1488
37. Kajiya M, Shiba H, Fujita T, Ouhara K, Takeda K, Mizuno N, Kawaguchi H, Kitagawa M, Takata T, Tsuji K, Kurihara H (2008) Brain-derived neurotrophic factor stimulates bone/cementum-related protein gene expression in cementoblasts. J Biol Chem 283:16259–16267
38. Chuderland D, Marmor G, Shainskaya A, Seger R (2008) Calcium-mediated interactions regulate the subcellular localization of extracellular signal-regulated kinases. J Biol Chem 283: 11176–11188
39. Liu HW, Yacobi R, Savion N, Narayanan AS, Pitaru S (1997) A collagenous cementum-derived attachment protein is a marker for progenitor of the mineralized tissue-forming cell lineage of the periodontal ligament. J Bone Miner Res 12:1691–1699
40. Hayami T, Zhang Q, Kapila Y, Kapila S (2007) Dexamethasone's enhancement of osteoblastic markers in human periodontal ligament cells is associated with inhibition of collagenase expression. Bone 40:93–104
41. Villarreal-Ramírez E, Moreno A, Mas-Oliva J, Chávez-Pacheco JL, Narayanan AS, Gil-Chavarría I, Zeichner-David M, Arzate H (2009) Characterization of recombinant human cementum protein 1 (rhCEMP1): primary role in biomineralization. Biochem Biophys Res Commun 384:49–54
42. Schild C, Beyeler M, Lang NP, Trueb B (2009) Cementum attachment protein/protein-tyrosine phosphotase-like member A is not expressed in teeth. Int J Mol Med 23:293–296